Conformity Experiment on Inelastic Scattering Exponent of Electrons in Two Dimensions

Ching-Chen Yeh[1,2,†] Pin-Chi Liao[2,†] Yanfei Yang,[1,3] Wei-Chen Lin,[1,4,5] Alireza R. Panna,[1] Albert F. Rigosi,[1] Randolph E. Elmquist,[1] and Chi-Te Liang[2,6,7,*]

[1]*National Institute of Standards and Technology (NIST), Gaithersburg, Maryland 20899, USA*
[2]*Department of Physics, National Taiwan University, Taipei 106, Taiwan*
[3]*Graphene Waves, Germantown, Maryland 20876, USA*
[4]*Taiwan International Graduate Program, Academia Sinica, Taipei 115, Taiwan*
[5]*Department of Engineering and System Science, National Tsing Hua University, Hsinchu 300, Taiwan*
[6]*Center for Quantum Science and Engineering (CQSE), National Taiwan University, Taipei 106, Taiwan*
[7]*Taiwan Consortium of Emergent Crystalline Materials (TCECM), Taipei 106, Taiwan*

The quantum Hall (QH) effect is one of the most widely studied physical phenomenon in two dimensions. The plateau-plateau transition within this effect can be comprehensively described by the scaling theory, which encompasses three pivotal exponents: the critical exponent κ, the inelastic scattering exponent p, and the universal exponent γ. Prior studies have focused on measuring κ and estimating γ, assuming a constant p value of 2 across magnetic fields. Here, our work marks a significant advancement by measuring all three exponents within a single graphene device and a conventional two-dimensional electron system. This study uniquely determines p at low magnetic fields (weak localization region and well outside the QH regime) and high magnetic fields (in the vicinity of the QH regime). Employing a comprehensive analytical approach that includes weak localization, plateau-plateau transitions, and variable range hopping, we have directly determined κ, p, and γ. Our findings reveal a distinct variation in p, shifting from 1 in the low magnetic field regime to 2 in the QH regime in graphene.

Introduction—The quantum Hall (QH) effect, which is a widely studied phenomenon across various two-dimensional (2D) systems, transcends the constraints of material specifics and disorder types. In the QH regime, electronic states are quantized into Landau levels, characterized by delocalized states at their centers and localized states at their boundaries. Scaling theory, serving as a fundamental framework [1,2], conceptualizes transitions between QH plateaus as localized-delocalized transitions, typifying quantum phase transitions with universal critical behavior.

According to the scaling theory, the localization length ξ diverges near the center of a Landau level (E_c), following a power-law relation $\xi \sim |E - E_c|^{-\gamma}$, where γ represents the universal exponent [1,2]. This relationship extends to variations in the applied magnetic field B, transforming into $\xi \sim |B - B_c|^{-\gamma}$. In real systems, this behavior is observable in the broadened density of states, as reflected in longitudinal and Hall resistivities (ρ_{xx} and ρ_{xy}). The finite scaling theory is formulated as $(B^{\max} - B_c) \sim T^\kappa$ [Ref. [3]] and $d\rho_{xy}/dB \sim T^{-\kappa}$, where $B^{\max}$ is the peak magnetic field position at different temperatures T, B_c is the critical

magnetic field, $\kappa = p/(2\gamma)$ is the critical exponent, and p is the inelastic scattering exponent, with $L_\phi \sim T^{-p/2}$ at finite temperatures representing the inelastic scattering length or phase coherence length [1,4].

Previous studies have rigorously examined critical behaviors in the plateau-plateau (P-P) transition, proposing their description through the scaling theory [1,2]. The critical exponent κ, subject to spin or valley degeneracy, has been reported as 0.42 ± 0.04 in spin-split systems [1,2] and 0.21 ± 0.02 in spin-degenerate systems [5]. Under the assumption that p equals 2 and is independent of B, the universal exponent γ has been determined to be $4/3$ for classical percolation [6,7] and $7/3$ for quantum percolation [8–10]. However, this assumption of $p = 2$ is debated [11], as it lacks justification in scenarios other than the clean limit, where $p = 1$ might be more appropriate. Moreover, those samples are high mobility and no signature of weak localization (WL) at low magnetic fields has been reported, hindering any possible measurements on the inelastic scattering exponent p in the low magnetic field regime [1,2,5]. Subsequent research revealed a broad spectrum of κ values $0.15 \leq \kappa \leq 0.81$ [Refs. [12–17]], challenging its universality and suggesting influences from varying disorder correlation lengths [13,14]. Recent theoretical work elaborates on the correspondence and highlights similar localization physics in the integer and fractional quantum

---

*Contact author: ctliang@phys.ntu.edu.tw
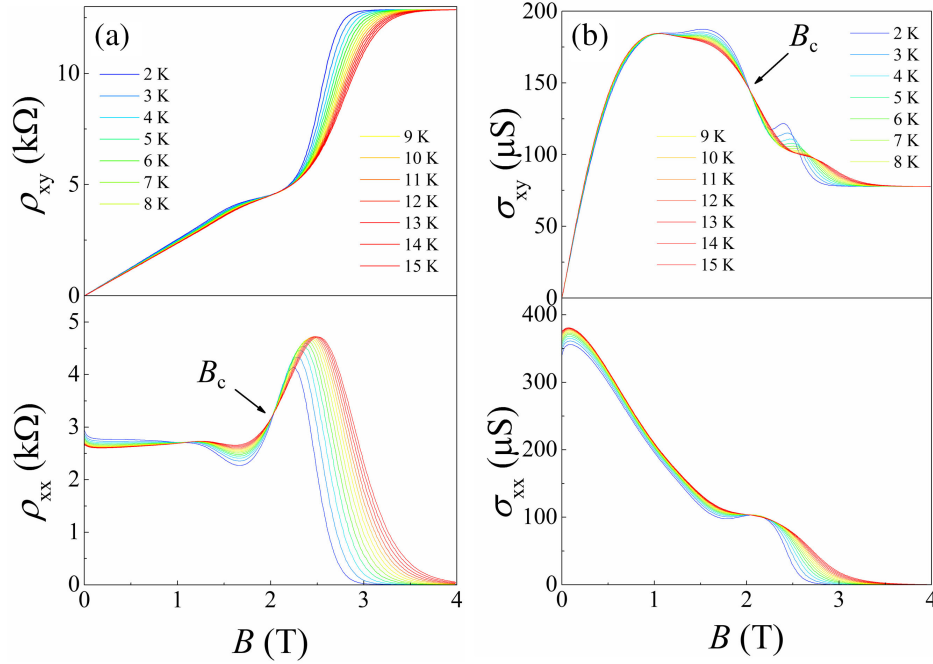†These authors contributed equally to this work.

FIG. 1.   (a) $\rho_{xy}(B)$ and $\rho_{xx}(B)$ at different temperatures (b) $\sigma_{xy}(B)$ and $\sigma_{xx}(B)$ at various temperatures.

Hall regimes [18]. Moreover, seminal work further addresses the nonuniversal κ in some plateau-plateau transitions in the fractional quantum Hall regime [19], pointing out several possible origins which deserve future investigations. Importantly, the exact value of p, particularly in high magnetic fields, has remained elusive, with its determination dependent on the mechanism of inelastic scattering of delocalized electrons.

Theoretical investigations predict diverse temperature dependencies under different physical conditions, leading to variations in the relationships among κ, γ, and p [20]. In diffuse transport [6,21], the relationship is $\kappa = 1/(2\gamma)$. For electron-electron scattering in pure metals, $\kappa = 2/\gamma$ is observed [22], while for electron-phonon scattering, $\kappa = p/\gamma$ with p ranging from 1.0 to 4.0 is proposed [6,21,23]. In scenarios involving noninteracting electrons, the quantum percolation model with Coulomb interaction suggests $\kappa = 1/\gamma$ [24], a relation also indicated for graphene, scattering on short-range potentials in variable range hopping conduction within Landau level (LL) tails broadened by disorder [25].

Here, we report significant contributions to the aforementioned research areas by unequivocally determining the inelastic scattering exponent p at low magnetic fields using WL analysis and at high magnetic fields near the QH regime using variable-range hopping (VRH) analysis, all within a single device. In order to achieve this, clear temperature-independent points in ρ_{xx} and σ_{xy} [26] as well as negative magnetoresistance near zero magnetic field are required. At low magnetic fields, the observation of negative magnetoresistivity, indicative of WL, facilitates

the extraction of L_ϕ and the inelastic scattering exponent $p = 1$, aligning with that in the dirty limit. Conversely, at high magnetic fields in the QH regime, a clear crossing point in the measured resistivity allows VRH analysis of the conductivity peak tail [27] to lead to the determination of γ. Notably, we draw upon recent important work reporting a substantially higher universal exponent ($\gamma \approx 2.6$ instead of $7/3$) of the Anderson transitions in the integer quantum Hall regime [28]. Combined with κ, derived from scaling analysis of P-P transitions, we ascertain the high-magnetic-field inelastic scattering exponent $p = 2$, characteristic of the clean limit. This variation in p underscores a transition of the device from the dirty limit to the clean limit, providing novel insights into the QH effect and its underlying mechanisms.

Experimental results—In our experiments, we employed epitaxial monolayer graphene grown on a semi-insulating 4H-SiC(0001) substrate. The graphene sample was shaped into a Hall bar geometry, with a length of 2000 µm and a width of 400 µm. Such a large-size sample is advantageous for studying weak localization and the QH effect. At $T = 2$ K, the carrier density and mobility of our graphene sample are determined to be 2.66×10^{11} cm^{-2} and 8950 cm^2 V^{-1} s^{-1}, respectively.

Magnetotransport measurements—As presented in Fig. 1(a), we extracted the symmetric and antisymmetric components to accurately probe these properties and avoid potential mixed contributions of ρ_{xx} and ρ_{xy} [29,30]. This extraction reveals a clear crossing point at $B_c = 2.03$ T in the longitudinal resistivity. (The measured magnetoresistivities are shown in Fig. S1 of the Supplemental Material
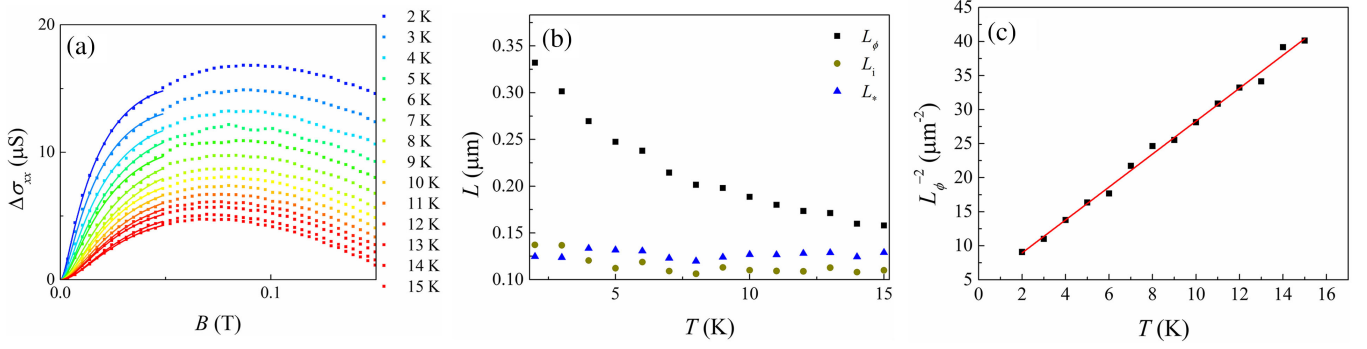
FIG. 2. (a) The converted magnetoconductivity in a low magnetic field regime. The solid symbols denote the experimental data, while the solid curves represent the theoretical fits based on the weak localization model. (b) Temperature dependence of three key lengths: the inelastic scattering length (L_ϕ), elastic intervalley scattering length (L_i), and elastic intravalley scattering length (L_*), showcasing how each varies with temperature. (c) The squared inverse of the inelastic scattering length (L_ϕ^{-2}) as it varies across different temperatures, demonstrating a linear relationship that follows the form $L_\phi \sim T^{-p/2}$.

[31]). In the absence of a magnetic field, ρ_{xx} increases with decreasing temperature, indicative of insulating properties typical of the diffusive regime.

Upon increasing the magnetic field, we observe a notable decrease in the slope of ρ_{xx} as ρ_{xy} approaches $h/(6e^2)$, signaling the onset of the $\nu = 6$ QH state. As the magnetic field is further increased beyond 3.5 T, a clear emergence of the $\nu = 2$ plateau is observed, signifying a transition from the $\nu = 6$ to the $\nu = 2$ QH state.

Figure 1(b) displays the magnetoconductivities, $\sigma_{xx} = \rho_{xx}/(\rho_{xx}^2 + \rho_{xy}^2)$ and $\sigma_{xy} = \rho_{xy}/(\rho_{xx}^2 + \rho_{xy}^2)$ at different temperatures T. The observed temperature dependence of the Hall slope $\delta\rho_{xy}/\delta B$ is attributed to electron-electron interactions [33], which significantly influence the transport properties of the system [Fig. 1(a)]. Notably, a temperature-independent crossing point at $B_c = 2.03$ T is also observed in Hall conductivity [Fig. 1(b)], consistent with the crossing point identified in longitudinal resistivity [Fig. 1(a)].

In Fig. 2(a), we present the converted magnetoconductivity, $\Delta\sigma_{xx} = \sigma_{xx}(B) - \sigma_{xx}(0)$, plotted against magnetic field. This data are analyzed using the formula derived by McCann et al. [34]:

$$\Delta\sigma_{xx}(B) = \frac{e^2}{\pi h}\left[F\left(\frac{8\pi B}{\frac{h}{e}L_\phi^{-2}}\right) - F\left(\frac{8\pi B}{\frac{h}{e}(L_\phi^{-2} + 2L_i^{-2})}\right) \right.$$
$$\left. - 2F\left(\frac{8\pi B}{\frac{h}{e}(L_\phi^{-2} + L_i^{-2} + L_*^{-2})}\right) \right], \quad (1)$$

where $F(z) = \ln z + \psi(0.5 + z^{-1})$ and $\psi(x)$ is the digamma function. Here, L_ϕ, L_i, and L_* represent the phase coherence length, elastic intervalley scattering length, and elastic intravalley scattering length, respectively. Utilizing Eq. (1), we extracted the temperature dependence of these characteristic lengths, as depicted in Fig. 2(b). Our analysis, refined through the three-parameter

fit results, emphasizes the importance of the first term associated with L_ϕ in our methodology. This approach allows for the accurate extraction of L_ϕ, essential for calculating the inelastic scattering exponent p from the temperature dependence of coherence, as demonstrated in Fig. 2(c). While L_i and L_* are integral to our theoretical model, in our fitting regime, their precise values are secondary to our study's main objective. The linear dependence of L_ϕ^{-2} on temperature (T) aligns with the relation $\tau_\phi^{-1} = \beta k_B T \ln g/\hbar g$, where $\tau_\phi = L_\phi^2/D$ and $g = \sigma_{xx} h/e^2$ [35]. The T dependence of L_ϕ^{-2} suggests that electron-electron scattering is the dominant mechanism for inelastic scattering, leading to an inelastic scattering length exponent $p = 1$. This result aligns with predictions for the dirty limit [36] and corroborates previous findings in both monolayer [37–39] and bilayer graphene [40].

Scaling analysis of the P-P transition—To investigate the scaling behavior associated with the $\nu = 6$ to $v = 2$ P-P transition, we analyzed two critical parameters plotted against temperature on a logarithmic scale, as shown in Fig. 3, including the maximum slope of the Hall resistivity $(d\rho_{xy}/dB)_{max}$ and the magnetic field width of the transition $\Delta B = B^{max} - B_c$ [3].

In our scaling analysis of the P-P transition, our findings indicate a critical exponent κ of 0.31 ± 0.01. This value of κ was derived from both the magnetic field width of the transition ΔB and the maximum slope of the Hall resistivity $(d\rho_{xy}/dB)_{max}$, shown in Figs. 3(a) and 3(b), respectively. Notably, our observed value of κ deviates from the commonly referenced universal value of approximately 0.42. This departure highlights the distinct scaling behavior observed in our study, setting it apart from previous findings. It is worth noting that this universal value of $\kappa \approx 0.42$, has been corroborated by Shen et al. [29], who interpreted their results as being consistent with the pioneering work by Wei et al. [1]. This deviation could be attributed to LL mixing effects in graphene [41]. Our

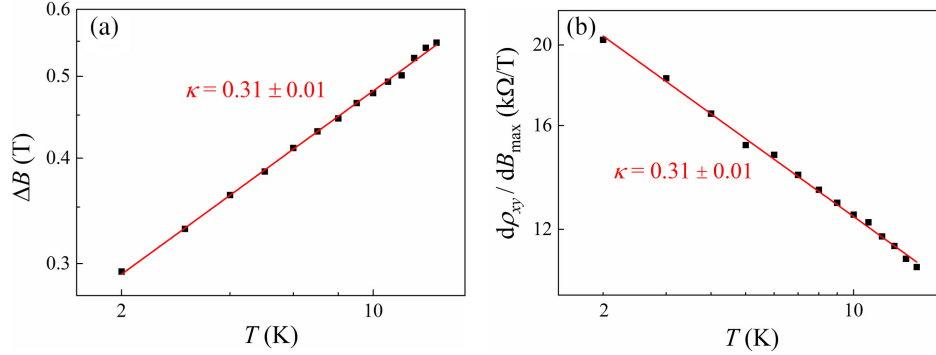FIG. 3.   (a) The magnetic field width of the transition ΔB. (b) The maximum slope of the Hall resistivity $(d\rho_{xy}/dB)_{max}$ versus T.

results on a wide range of κ in epitaxial graphene on SiC ($0.31 \leq \kappa \leq 0.74$; also see Supplemental Material [31]) may suggest a nonuniversal κ, and importantly, provide the first test of the theoretical model [3] in graphene.

Variable range hopping analysis—VRH analysis stands as a pivotal component of our study, offering a contrast to previous methodologies that relied on size-dependent measurements, such as those utilized in GaAs/AlGaAs heterostructures [42]. Those earlier methods could be limited by the sample's dimensions when deducing the inelastic scattering exponent p. Our approach, utilizing VRH, allows for the determination of p without such sample size constraints, making it applicable to a wide variety of samples across different 2D systems, though clear T-independent points in ρ_{xx} and σ_{xy} at B_c are needed.

At low temperatures, where VRH becomes the predominant transport mechanism in localized regions, the Coulomb interaction between localized electrons notably creates a Coulomb gap in the density of states near the Fermi level [43]. This behavior is described by the following expression:

$$\sigma_{xx}(T) \propto \frac{1}{T} e^{-\sqrt{\frac{T_0}{T}}}, \qquad (2)$$

where

$$k_B T_0 = C \frac{e^2}{4\pi\varepsilon\varepsilon_0 \xi(B)}. \qquad (3)$$

In Eq. (3), T_0 denotes the characteristic temperature, with C as a constant of order unity and ε representing the permittivity of the sample. In our analysis of the $\nu = 6$ to $v = 2$ transition of σ_{xx} (Refs. [24,43–45]), we scrutinize the tail of the conduction peak ($2.7\ \text{T} < B < 3.5\ \text{T}$) to extract the scaling exponent γ [27,46]. This methodological choice, while traditionally employed for its direct approach in scaling analyses, acknowledges the nuanced role of LL mixing across the studied magnetic field range.

In Fig. 4(a), we plotted $\sigma_{xx}T$ against $T^{1/2}$ for various magnetic fields, observing high linearity at higher temperatures with a slope corresponding to $-\sqrt{T_0}$.

Deviations at lower temperatures ($T < 5$ K) may be attributed to high T_0 values relative to T. Utilizing scaling theory, where ξ is proportional to $|B - B_c|^{-\gamma}$, we derived $\gamma = 3.19 \pm 0.03$ from a logarithmic plot of T_0 against $1/B_c - 1/B$, as shown in Fig. 4(b). This value deviates from the expected universal value of 7/3 predicted by the quantum percolation model [47]. The observations of higher γ and lower κ values, consistent with other studies [48], and the deviation of κ from its universal value could be attributed to factors such as LL mixing [41].
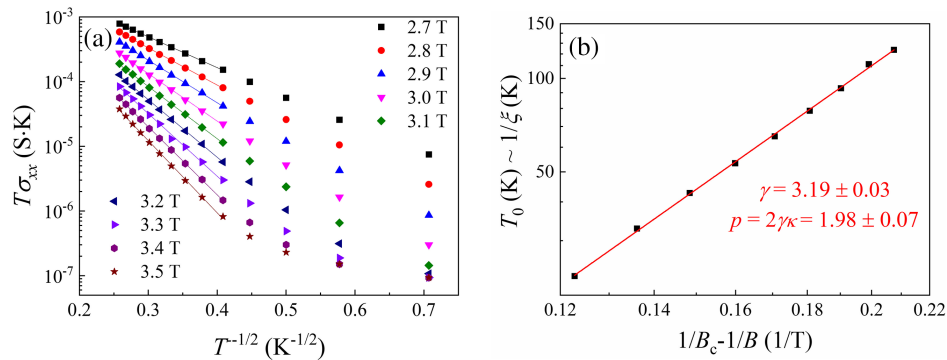

FIG. 4.   (a) Semilogarithmic plot demonstrating the $T^{-\frac{1}{2}}$ dependence of $\sigma_{xx} \cdot T$, specifically focusing on the tail region of the $\nu = 2$ to $\nu = 6$ transition peak. (b) The characteristic temperature T_0, extracted from the slopes observed in part (a) as a function of $1/B_c - 1/B$.

Remarkably, our VRH analysis facilitates the estimation of $p \approx 2$ through the relationship $\kappa = p/(2\gamma)$, a significant contrast to the value $p = 1$ observed at lower magnetic fields.

Discussion and conclusion—In this final section, we contextualize our experimental results with the broader research spectrum on various 2D systems such as InGaAs/InP and $Al_xGa_{1-x}As$/GaAs heterostructures. Wei *et al.* [1] studied InGaAs/InP heterostructures and initially proposed the concept of universal scaling in two dimensions. They suggested that with a fixed $p = 2$, the critical exponent κ should be a universal constant, independent of LL.

In contrast, Koch *et al.* [12] examined low-mobility $Al_xGa_{1-x}As$/GaAs heterostructures, revealing scaling behavior with nonuniversal κ values dependent on mobility. These variations could stem from long-range interactions [14] or differences in the inelastic scattering exponent p across samples [42]. They aligned their findings with the quantum percolation model, showing a possible universal exponent $\nu = 2.3 \pm 0.1$ at the lowest LLs and varied p values ranging from 2.7 ± 0.3 to 3.4 ± 0.4 determined through size-dependent methods.

In addition to the work on graphene Corbino device [48], earlier studies on GaAs-based heterostructures [49] measured $\kappa = 0.50 \pm 0.03$ and extracted $\gamma \approx 2$ using VRH. Despite deviating from expected norms, these values were rationalized within scaling theory, assuming $p = 2$. The dominance of different VRH mechanisms, such as Efros-Shklovskii (E-S) VRH and Mott VRH, under varying magnetic field conditions was noted [50].

Addressing concerns from a previous study [14] regarding nonuniversal values potentially arising from nonoptimal temperatures or self-heating effects due to high excitation currents, we ensured that our experimental setup and conditions were robust against such issues. Notably, self-heating was rigorously verified not to significantly impact our measurements (detailed in Supplemental Material, Sec. II [31]).

In our study, we have innovatively advanced methodologies to extract three critical scaling exponents within a single device, a contrast to previous approaches [42]. This advancement allows for the precise and reliable determination of the inelastic scattering exponent p at low magnetic fields outside the QH regime and at high magnetic fields within the QH regime, a capability previously unattainable.

Our analysis reveals a distinct value of $p = 1$ in the low magnetic field regime, determined through WL analysis. Importantly, our study extends to examine two additional graphene devices that exhibit the insulator-quantum Hall transition [51], offering further support for our conclusions (see Supplemental Material, Sec. III for details [31]). This finding contrasts with $p \approx 2$ in the high magnetic field regime, highlighting a significant transition from the dirty

TABLE I. Comparison of inelastic scattering exponents p in epitaxial graphene and GaAs-based 2DEG under different magnetic field conditions.

	Low magnetic fields	High magnetic fields
Epitaxial graphene	$p \approx 1$	$p \approx 2$
GaAs-based 2DEG	$p \approx 1$	$p \approx 1$

limit to the clean limit. Within the QH region, the observed inelastic exponent $p \approx 2$ underscores notable differences in scattering mechanisms between the low magnetic field regime and the tail of LLs, where carrier transport predominantly occurs through edge states and the inelastic scattering rate of electrons is markedly suppressed [52].

Conversely, our investigations of the GaAs/AlGaAs heterostructure [53] revealed a consistent value of $p \approx 1$ at high magnetic fields within the QH regime, as detailed in Supplemental Material, Sec. IV [31]. For low magnetic fields, we used WL analysis outside the QH regime. This variation underscores the need for a meticulous derivation of p value within the QH regime, considering its sensitivity to magnetic field strength. For clarity, the exponents between graphene and GaAs are compared as outlined in Table I.

The distinctive p values observed in studies by Koch *et al.* [12] and Wei *et al.* [1,5] are rationalized in this context, acknowledging the varying influence of the bulk state on transport, contingent on the strength of electron-electron scattering [20,48,54]. It is worth noting that while many studies typically assume $p = 2$, several works have determined p through size-dependent measurement or approximation methods. Therefore, Table II summarizes these results, illustrating the variance in p values across different mobilities in GaAs-based 2DEG devices.

While L_ϕ and its power-law dependencies have been well characterized in the critical regime for QH systems, a comprehensive study of p within the quantum critical regime has been somewhat limited. Our systematic efforts in this study address this research gap by probing p at low

TABLE II. Comparison of inelastic scattering exponents p in GaAs-based 2DEG across different mobilities.

Method	$\mu(cm^2/Vs)$	p	Ref.
Using $p = 2\kappa\gamma$	1.01×10^4	$p = 1$	This work
Using $p = 2\kappa\gamma$	1.5×10^5	$p = 2$	[49]
Using $p = 2\kappa\gamma$	4.1×10^5	$p = 2$	[41]
Sample-size dependence measurement	1.5×10^5	$p = 3.0 - 3.4$	[42]
	5.8×10^4	$p = 2.7 - 3.3$	
Assumption of zero temperature fluctuations	2.9×10^5	$p = 1.5 - 2.1$	[30]
Sample-size dependence measurement	$\approx 10^6$	$p = 2$	[22,23]

magnetic fields outside the QH regime and at high magnetic fields within the QH regime. Conducted on monolayer graphene, a true 2D system, our results are not influenced by long-range interactions [13,14], enabling us to focus exclusively on the mechanisms of electron scattering. Various systems may be useful for further investigations [55–57].

In conclusion, our investigation into the QH P-P transition and the extraction of three critical exponents provide substantial experimental insights into scaling behavior and, specifically, inelastic scattering in two dimensions. While reviewing experimental and theoretical works, we observe that κ and p may deviate from conventional values, and propose that the nonuniversal scaling behavior is still governed by the relation $\kappa = p/(2\gamma)$. Variations in exponents could be attributed to differences in sample characteristics, such as impurity type, distribution, and geometry [58]. Central to our findings is the inelastic scattering exponent p, determined by the dominant mechanism of electron scattering and undiminished by the perturbative effects, including possible LL mixing. A significant achievement of our current study is the extraction of these exponents within a single device across two distinct 2D systems. This accomplishment not only highlights the essence of our work but also sets a new benchmark for future research in this field. Our findings pave the way for further exploration and a deeper understanding of the complex behaviors in 2D material systems.

[1] H. P. Wei, D. C. Tsui, M. A. Paalanen, and A. M. M. Pruisken, Experiments on delocalization and universality in the integral quantum Hall effect, Phys. Rev. Lett. **61**, 1294 (1988).

[2] A. M. M. Pruisken, Universal singularities in the integral quantum Hall effect, Phys. Rev. Lett. **61**, 1297 (1988).

[3] A. M. M. Pruisken, Topological principles in the theory of Anderson localization, Int. J. Mod. Phys. B **24**, 1895 (2010).

[4] B. Huckestein, Scaling theory of the integer quantum Hall effect, Rev. Mod. Phys. **67**, 357 (1995).

[5] S. W. Hwang, H. P. Wei, L. W. Engel, D. C. Tsui, and A. M. M. Pruisken, Scaling in spin-degenerate Landau levels in the integer quantum Hall effect, Phys. Rev. B **48**, 11416 (1993).

[6] J. T. Chalker and P. D. Coddington, Percolation, quantum tunnelling, and the integer Hall effect, J. Phys. C **21**, 2665 (1988).

[7] B. Huckestein and B. Kramer, One-parameter scaling in the lowest Landau band: Precise determination of the critical behavior of the localization length, Phys. Rev. Lett. **64**, 1437 (1990).

[8] D.-H. Lee, Z. Wang, and S. Kivelson, Quantum percolation and plateau transitions in the quantum Hall effect, Phys. Rev. Lett. **70**, 4130 (1993).

[9] S. A. Trugman, Localization, percolation, and the quantum Hall effect, Phys. Rev. B **27**, 7539 (1983).

[10] B. Kramer, T. Ohtsuki, and S. Kettemann, Random network models and quantum phase transitions in two dimensions, Phys. Rep. **417**, 211 (2005).

[11] S. Das Sarma and D. Liu, Scaling behavior of the activated conductivity in a quantum Hall liquid, Phys. Rev. B **48**, 9166 (1993).

[12] S. Koch, R. J. Haug, K. v. Klitzing, and K. Ploog, Experiments on scaling in $Al_xGa_{1-x}As$/GaAs heterostructures under quantum Hall conditions, Phys. Rev. B **43**, 6828 (R) (1991).

[13] W. Li, G. A. Csáthy, D. C. Tsui, L. N. Pfeiffer, and K. W. West, Scaling and universality of integer quantum Hall plateau-to-plateau transitions. Phys. Rev. Lett. **94**, 206807 (2005).

[14] H. P. Wei, S. Y. Lin, D. C. Tsui, and A. M. M. Pruisken, Effect of long-range potential fluctuations on scaling in the integer quantum Hall effect, Phys. Rev. B **45**, 3926 (1992).

[15] X. Kou, L. Pan, J. Wang, Y. Fan, E. S. Choi, W.-L. Lee, T. Nie, K. Murata, Q. Shao, S.-C. Zhang, and K. L. Wang, Metal-to-insulator switching in quantum anomalous Hall states, Nat. Commun. **6**, 8474 (2015).

[16] P. Deng, C. Eckberg, P. Zhang, G. Qiu, E. Emmanouilidou, G. Yin, S. K. Chong, N. Tai, N. Ni, and K. L. Wang, Probing the mesoscopic size limit of quantum anomalous Hall insulators, Nat. Commun. **13**, 4246 (2022).

[17] X. Wu, D. Xiao, C.-Z. Chen, J. Sun, L. Zhang, M. H. W. Chan, N. Samarth, X. C. Xie, X. Lin, and C.-Z. Chang, Scaling behavior of the quantum phase transition from a quantum-anomalous-Hall insulator to an axion insulator, Nat. Commun. **11**, 4532 (2020).

[18] S. Pu, G. J. Sreejith, and J. K. Jain, Anderson localization in the fractional quantum Hall effect, Phys. Rev. Lett. **128**, 116801 (2022); **131**, 079904(E) (2023).

[19] P. T. Madathil, K. A. Villegas Rosales, C. T. Tai, Y. J. Chung, L. N. Pfeiffer, K. W. West, K. W. Baldwin, and M. Shayegan, Delocalization and universality of the fractional quantum Hall plateau-to-plateau transitions, Phys. Rev. Lett. **130**, 226503 (2023).

[20] Y. G. Arapov, S. V. Gudina, E. V. Deryushkina, N. G. Shelushinina, and M. V. Yakunin, On the issue of universality of critical exponents in the quantum Hall effect mode, Low Temp. Phys. **45**, 181 (2019).

[21] M. B. Isichenko, Percolation, statistical topography, and transport in random media, Rev. Mod. Phys. **64**, 961 (1992).

[22] W. Li, J. S. Xia, C. Vicente, N. S. Sullivan, W. Pan, D. C. Tsui, L. N. Pfeiffer, and K. W. West, Crossover from the nonuniversal scaling regime to the universal scaling regime in quantum Hall plateau transitions, Phys. Rev. B **81**, 033305 (2010).

[23] W. Li, C. L. Vicente, J. S. Xia, W. Pan, D. C. Tsui, L. N. Pfeiffer, and K. W. West, Scaling in plateau-to-plateau transition: A direct connection of quantum Hall systems with the Anderson localization model, Phys. Rev. Lett. **102**, 216801 (2009).

[24] F. Hohls, U. Zeitler, and R. J. Haug, Hopping conductivity in the quantum Hall effect: Revival of universal scaling. Phys. Rev. Lett. **88**, 036802 (2002).

[25] D. G. Polyakov and B. I. Shklovskii, Variable range hopping as the mechanism of the conductivity peak broadening in the quantum Hall regime. Phys. Rev. Lett. **70**, 3796 (1993).

[26] R. J. F. Hughes, J. T. Nicholls, J. E. F. Frost, E. H. Linfield, M. Pepper, C. J. B. Ford, D. A. Ritchie, G. A. C. Jones, E. Kogan, and M. Kaveh, Magnetic-field-induced insulator-quantum Hall-insulator transition in a disordered two-dimensional electron gas, J. Phys. Condens. Matter **6**, 4763 (1994).

[27] Y. Ono, Localization of electrons under strong magnetic fields in a two-dimensional system, J. Phys. Soc. Jpn. **51**, 237 (1982).

[28] E. J. Dresselhaus, B. Sbierski, and I. A. Gruzberg, Scaling collapse of longitudinal conductance near the integer quantum Hall transition, Phys. Rev. Lett. **129**, 026801 (2022).

[29] T. Shen, A. T. Neal, M. L. Bolen, J. Gu, L. W. Engel, M. A. Capano, and P. D. Ye, Quantum-Hall plateau-plateau transition in top-gated epitaxial graphene grown on SiC (0001), J. Appl. Phys. **111**, 013716 (2012).

[30] M. Hilke, D. Shahar, S. H. Song, D. C. Tsui, Y. H. Xie, and D. Monroe, Experimental evidence for a two-dimensional quantized Hall insulator, Nature (London) **395**, 675 (1998).

[31] See Supplemental Material at http://link.aps.org/supplemental/10.1103/PhysRevLett.133.096302 for details on measured results, self-heating investigation, inelastic scattering exponent p at low magnetic field, and analysis in GaAs/AlGaAs heterostructure, which includes Ref. [32].

[32] S. Hikami, A. I. Larkin, and Y. Nagaoka, Spin-orbit interaction and magnetoresistance in the two dimensional random system, Prog. Theor. Phys. **63**, 707 (1980).

[33] C.-W. Liu, C. Chuang, Y. Yang, R. E. Elmquist, Y.-J. Ho, H.-Y. Lee, and C.-T. Liang, Temperature dependence of electron density and electron–electron interactions in monolayer epitaxial graphene grown on SiC, 2D Mater. **4**, 025007 (2017).

[34] E. McCann, K. Kechedzhi, V. I. Fal'ko, H. Suzuura, T. Ando, and B. L. Altshuler, Weak-localization magnetoresistance and valley symmetry in grapheme, Phys. Rev. Lett. **97**, 146805 (2006).

[35] B. L. Altshuler, A. G. Aronov, and D. E. Khmelnitsky, Effects of electron-electron collisions with small energy transfers on quantum localization, J. Phys. C **15**, 7367 (1982).

[36] E. Abrahams, P. W. Anderson, P. A. Lee, and T. V. Ramakrishnan, Quasiparticle lifetime in disordered two-dimensional metals, Phys. Rev. B **24**, 6783 (1981).

[37] F. V. Tikhonenko, D. W. Horsell, R. V. Gorbachev, and A. K. Savchenko, Weak localization in graphene flakes, Phys. Rev. Lett. **100**, 056802 (2008).

[38] S. Pezzini, C. Cobaleda, E. Diez, and V. Bellani, Quantum interference corrections to magnetoconductivity in grapheme, Phys. Rev. B **85**, 165451 (2012).

[39] C.-C. Yeh, P.-C. Liao, D. K. Patel, W.-C. Lin, S.-C. Wang, A. F. Rigosi, R. E. Elmquist, and C.-T. Liang, Direct insulator to relativistic quantum Hall transition in grapheme, Phys. Rev. B **108**, 205304 (2023).

[40] R. V. Gorbachev, F. V. Tikhonenko, A. S. Mayorov, D. W. Horsell, and A. K. Savchenko, Weak localization in bilayer grapheme, Phys. Rev. Lett. **98**, 176805 (2007).

[41] Y. J. Zhao, T. Tu, X. J. Hao, G. C. Guo, H. W. Jiang, and G. P. Guo, Experimental studies of scaling behavior of a quantum Hall system with a tunable Landau level mixing, Phys. Rev. B **78**, 233301 (2008).

[42] S. Koch, R. J. Haug, K. v. Klitzing, and K. Ploog, Size-dependent analysis of the metal-insulator transition in the integral quantum Hall effect, Phys. Rev. Lett. **67**, 883 (1991).

[43] A. L. Efros and B. I. Shklovskii, Coulomb gap and low temperature conductivity of disordered systems, J. Phys. C **8**, L49 (1975).

[44] D. G. Polyakov and B. I. Shklovskii, Conductivity-peak broadening in the quantum Hall regime, Phys. Rev. B **48**, 11167 (1993).

[45] Y. Ono, Energy dependence of localization length of two-dimensional electron system moving in a random potential under strong magnetic fields, J. Phys. Soc. Jpn. **51**, 2055 (1982).

[46] I. Sodemann and A. H. MacDonald, Landau level mixing and the fractional quantum Hall effect, Phys. Rev. B **87**, 245425 (2013).

[47] G. V. Mil'nikov and I. M. Sokolov, Semiclassical localization in a magnetic field, Pis'ma Zh. Eksp. Teor. Fiz. **48**, 494 (1988) [JEPT Lett. **48**, 536 (1988)], http://jetpletters.ru/ps/1109/article_16776.shtml.

[48] E. C. Peters, A. J. M. Giesbers, M. Burghard, and K. Kern, Scaling in the quantum Hall regime of graphene Corbino devices, Appl. Phys. Lett. **104**, 203109 (2014).

[49] K.-H. Yoo, H. C. Kwon, and J. C. Park, Experiments on scaling and variable range hopping in the integral quantum Hall effect, Solid State Commun. **92**, 821 (1994).

[50] Y.-C. Lee, C.-I. Liu, Y. Yang, R. E. Elmquist, and C.-T. Liang, Crossover from Efros-Shklovskii to Mott variable range hopping in monolayer epitaxial graphene grown on SiC, Chin. J. Phys. **55**, 1235 (2017).

[51] L.-I. Huang, Y. Yang, R. E. Elmquist, S.-T. Lo, F.-H. Liu, and C.-T. Liang, Insulator-quantum Hall transition in monolayer epitaxial grapheme, RSC Adv. **6**, 71977 (2016).

[52] T. Martin and S. Feng, Suppression of scattering in electron transport in mesoscopic quantum Hall systems, Phys. Rev. Lett. **64**, 1971 (1990).

[53] C.-C. Yeh, S.-C. Wang, S.-T. Lo, G.-H. Kim, D. A. Ritchie, G. Strasser, and C.-T. Liang, Quantum Hall plateau-plateau transition revisited, Chin. J. Phys. **82**, 149 (2023).

[54] H. P. Wei, L. W. Engel, and D. C. Tsui, Current scaling in the integer quantum Hall effect, Phys. Rev. B **50**, 14609 (1994).

[55] D. Weisshaupt, H. S. Funk, M. Oehme, D. Bloos, F. Berkmann, L. Seidel, I. A. Fischer, and J. Schulze, High mobility Ge 2DHG based MODFETs for low-temperature applications, Semicond. Sci. Technol. **38**, 035007 (2023).

[56] D. Alberto, Engineering the insulator-to-metal transition by tuning the population of dopant defects: First principles simulations of Se hyperdoped Si, Semicond. Sci. Technol. **38**, 014002 (2023).

[57] J.-H. Chen, J.-Y. Lin, J.-K. Tsai, H. Park, G.-H. Kim, D. H. Youn, H.-I. Cho, E.-J. Lee, J.-H. Lee, C.-T. Liang, and Y. F. Chen, Experimental evidence for Drude-Boltzmann-like transport in a two-dimensional electron gas in an AlGaN/GaN heterostructure, J. Korean Phys. Soc. **48**, 1539 (2006), https://www.jkps.or.kr/journal/view.html?spage=1539&volume=48&number=6.

[58] J. J. Lin and J. P. Bird, Recent experimental studies of electron dephasing in metal and semiconductor mesoscopic structures. J. Phys. Condens. Matter **14**, R501 (2002).